Available online at www.sciencedirect.com
ScienceDirect
Journal of the European Ceramic Society 29 (2009) 2079–2085
www.elsevier.com/locate/jeurceramsoc

Synthesis and characterization of continuous freestanding silicon carbide films with polycarbosilane (PCS)

Rongqian Yao[a,b,c], Zude Feng[a,b,*], Yuxi Yu[a], Siwei Li[a,b,c], Lifu Chen[a,b], Ying Zhang[a,b]

[a] Fujian Key Laboratory of Advanced Materials, Xiamen University, Xiamen 361005, China
[b] Department of Materials Science and Engineering, College of Materials, Xiamen University, Xiamen 361005, China
[c] College of Chemistry and Chemical Engineering, Xiamen University, Xiamen 361005, China

Received 28 July 2008; received in revised form 17 November 2008; accepted 24 November 2008
Available online 14 January 2009

Abstract

A technique based on melt spinning of precursor was introduced to produce continuous freestanding SiC films. An equipment including spinneret, mandril, tank and seal groove was designed and manufactured for melt spinning. The polycarbosilane (PCS) precursors were deaerated, melt spun, crosslinked (by oxidation or irradiation), and pyrolyzed at high temperature in order to convert the initial PCS into freestanding SiC films. Our results revealed that the continuous freestanding SiC films, approximately 8 μm to 190 μm in thickness depended on setting, were uniform and dense. Their microstructure consisted of amorphous SiO_xC_y, β-SiC nano-crystals and free carbon. The photoluminescence (PL) spectrum showed two blue emissions at 416 nm and 435 nm. The continuous freestanding SiC films with high modulus, high density, high surface hardness and optoelectronic properties may have potential applications in microelectromechanical systems (MEMS), advanced optoelectronic devices and such complex-shaped materials.
© 2008 Elsevier Ltd. All rights reserved.

Keywords: Freestanding SiC films; Oxidation-induced crosslinking; Electron beam irradiation; Microstructure; Photoluminescence

1. Introduction

Silicon carbide (SiC) films are currently being explored as an important ceramic coatings because of their hardness and toughness, which makes them a very attractive candidate material for scratch-resistant coatings on metals, glass, and other materials.[1–3] SiC films could also be used as a material for the next generation of high-power, high-temperature electronic and optoelectronic devices.[4] Amorphous and polycrystalline β-SiC films had attracted much attention for the applications such as hard protective coatings, semiconductor, structural materials for power microelectromechanical systems (MEMS) in harsh environments. SiC films are promising for these applications due to their large energy gap, high electric breakdown field, electron saturation drift velocity, high mobility, high thermal conductivity, chemical inertness and temperature stability.[4,5] In addition, SiC films are also a very good luminescent material emitting in the visible spectrum ranging from blue to yellow.[6] So far, chemical vapor deposition (CVD), physical vapor deposition (PVD), molecular beam epitaxy, sputtering, or laser ablation have been successfully employed to deposit SiC coatings on substrates.[3–6] However, these methods, based on relatively expensive equipment and time-consuming procedures, are not always practical or cost-efficient. It has been generally reported that the formation of voids and defects are observed at the SiC/substrate interface in the initial stage of the growth, which leads to serious problems in the realization of SiC MEMS devices.[7] In addition, the performance of the SiC coatings is often dependent on the coating/substrate interaction since the mismatches of thermal expansion coefficient and lattice constant usually exist at the interface. And residual strain accumulated at the interface can lead to warping problems. Therefore, there has been a considerable amount of interest in the development of alternative technique for producing SiC films which may avoid the significant difference of the thermal expansion coefficients between SiC and substrate.

* Corresponding author at: Department of Materials Science and Engineering, College of Materials, Xiamen University, 422 Siming South Road, Xiamen 361005, China. Tel.: +86 592 2181538; fax: +86 592 2183937.
E-mail address: zdfeng@xmu.edu.cn (Z. Feng).

0955-2219/$ – see front matter © 2008 Elsevier Ltd. All rights reserved.
doi:10.1016/j.jeurceramsoc.2008.11.019

Polycarbosilane (PCS), the precursor of continuous SiC fiber, is synthesized from polydimethylsilane (PDMS). It was first introduced by Yajima et al.[8] in 1975 and widely known for its use in the synthesis of Nicalon™ and Hi-Nicalon™ fibers. In the fiber fabrication process, the PCS is melt spun, cured with oxidation-induced crosslinking or electron beam (EB) irradiation, and then pyrolyzed at high temperature. This method is of great advantages in simple process, low cost and good performance.[9]

Chu et al.[10,11] first studied preparation and characterization of amorphous SiC film by a liquid route. In the SiC thin-film deposition process, the PCS was dissolved in a suitable solvent, cast onto the substrate, and then pyrolyzed. Because thin films of PCS were likely to be more sensitive to the pyrolysis conditions than fibers or bulk material, Colombo et al.[12,13] reported that PCS thin films were deposited on silicon substrates by spin casting and pyrolyzed under vacuum at temperature ranging from 200 °C to 1200 °C. At temperature ranging from 1000 °C to 1200 °C, the initial amorphous PCS films transformed to polycrystalline β-SiC. PCS films could be deposited at thickness up to 2 μm. However, extensive cracking existed in the pyrolyzed films and their thickness was limited after each deposition. Multiple-coating process was required to increase the thickness of the films. Mismatches of thermal expansion coefficient and lattice constant in the film/matrix interface still existed, although this technology could provide the possibility of coating large surfaces, objects with irregular geometries, and/or textile fibers. This meant that spin cast films had an inherently high residual stress and bad adhesion. Spin cast films were also less dense and more susceptible to chemical attack than materials deposited by other means.[14]

Nagasawa and Yagi had developed a low temperature process (1000 °C) to facilitate the growth of β-SiC films on 150 mm Si wafers. Recently, they managed to increase the SiC deposition rate by about 50 times as compared to the standard process, permitting the realization of thick freestanding β-SiC films after removing the Si substrate.[15] However, the technique could not avoid the formation of voids and defects at the SiC/Si interface.

Furthermore, some works on making MEMS from preceramic polymers had been reported. Silicon-based polymers containing nitrogen, carbon, boron, etc. had been developed as precursors for various non-oxide ceramics (SiC, Si_3N_4, different stoichiometric Si–C–N and Si–B–C–N system). Preceramic polymers could be utilized as reactive feedstock in microcasting technique, which involved the using of a mask generated by photolithography, subsequent casting, and the thermal or photochemical curing of the precursor compound. The method was reported to be more actual for the fabrication of MEMS.[16–26]

However, to the knowledge of the authors, there is no report concerning the preparation of continuous freestanding SiC films. Continuous freestanding films could avoid the coating/substrate interaction resulted from the techniques mentioned above. And the vital questions relating the technique are the uniformity, compactness and continuity of the resulted freestanding films.

In the present study, a special spinneret was designed and manufactured for melt spinning of PCS continuous freestanding films. Moreover, the precursor PCS green films were cured to be infusible with oxidation-induced crosslinking and electron beam irradiation, respectively. Subsequently the cured PCS films were pyrolyzed into inorganic material in regular-grade argon. The goal of this study was to develop a novel technology of preparing continuous freestanding SiC films by melt spinning of precursor. The morphology, microstructure and composition of the green and resulted films were characterized to provide a detailed understanding of technique and products.

2. Experimental procedure

The PCS samples (Si: 41.03 wt%, C: 43.24 wt%, O: 1.05 wt%) employed in this study were synthesized in our laboratory. They were transparent solid with a number average molecular weight of 1426 and a weight average molecular weight of 3296. The melting point of PCS was 215 °C and the chemical structure was represented below.

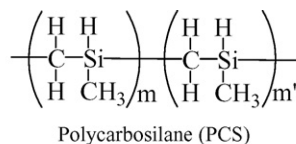

Polycarbosilane (PCS)

A schematic diagram of experimental equipment was shown in Fig. 1(a and b). A special spinneret was set up for melt spinning of films under heating condition. The experimental apparatus including spinneret, mandril, tank, seal cover and seal groove. A melt spinning machine was built for loading and spinning. The spinneret which was made of carbon steel contained four adjustment screws, spinneret mouth and double special-shaped spinneret blocks. The thickness of freestanding films was controlled by adjusting the spout size of the spinneret mouth and spinning speed. PCS samples were placed in the tank between the mandril and spinneret in order to spin the continuous freestanding green films through spinneret mouth.

PCS was first deaerated for 3 h in the vacuum deaeration furnace under 290 °C, and then melt spun using a melt spinning machine under 265 °C at an extrusion rate of 0.3 mm/min. The melting tank was protected with high-purity nitrogen to prevent the PCS from oxidation. The PCS green films were melt spun in air as PCS was extruded through the spinneret mouth. The spinning speed ranged from 100 m/min to 500 m/min with the different spout sizes (50 μm, 100 μm, 150 μm, 200 μm and 250 μm) of the spinneret mouth, respectively. The melt spun PCS green films were wound onto several coils, each coil contained freestanding films greater than 100 m in length. Some green films were treated with oxidation-induced crosslinking in an air at a flow rate of 200 ml/min with a heating rate of 3 °C/min and held for 3 h at 190 °C. The cured PCS films were pyrolyzed in an argon at a flow rate of 200 ml/min with a heating rate of 10 °C/min and held for 2 h at 1200 °C; other green films were irradiated by 2 MeV EB from an electron accelerator (Model GJ-2, Shanghai No. 1 Machine Tool Works, China) up to the dose of 12 MGy under the He atmosphere at room temperature with the radiation dose rate of 1.5 kGy/s. After the irradiation, the cured green films were heat-

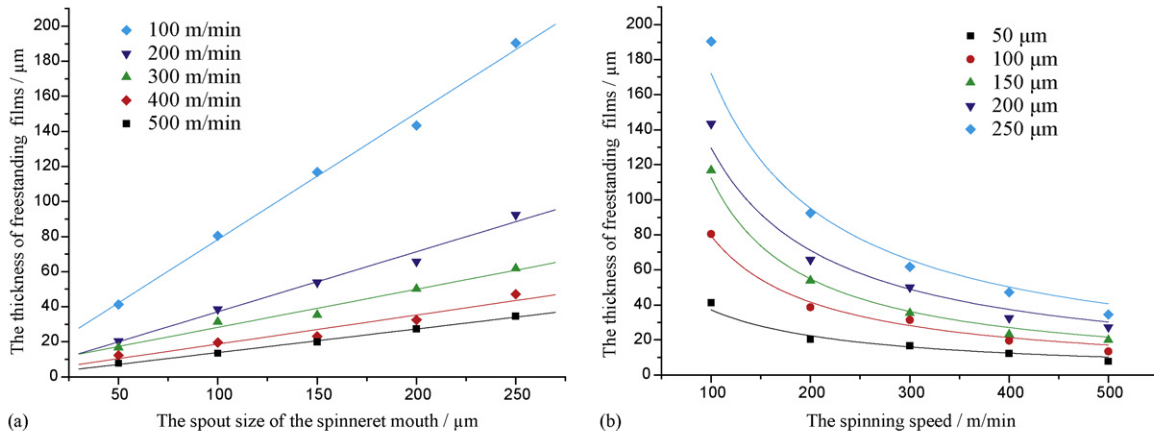

Fig. 1. The relationship among the thickness of the films, the spout size of the spinneret mouth and the spinning speed at an steady extrusion rate of 0.3 mm/min. (a) thickness as a function of the spout size of the spinneret mouth and (b) thickness as a function of the spinning speed.

treated at 400 °C for 1 h to quench the surviving free radicals produced by the irradiation in the films, because these free radicals were easy to react with oxygen in air, and reduced the heat resistance of the ceramic films obtained.[27,28] And then the cured PCS films were pyrolyzed in an argon at a flow rate of 200 ml/min with a heating rate of 10 °C/min and held for 2 h at 1200 °C. The morphology and thickness of the films were examined by a scanning electron microscope (SEM) (Model 1530, LEO, Germany), and their composition and microstructure were characterized by electron probe microanalysis (EPMA) (JXA-8100, JEOL, Japan), Fourier transform infrared spectrometer (Nicolet Avatar FT-IR 360, USA), Raman spectrometer (LabRam I, Dilor, France), transmission electron microscope (TEM) (Tecnai F30, Philips-FEI, USA) and X-ray diffractometer (XRD) (X'pert PRO, Panalytical, Netherlands). The typical physical properties of films were tested by Automatic Bridge (HP16047A, USA), Microhardness Tester (HV-1000, Nboeo Detecting Instrument, China) and Universal Testing Machine (Sun 2500, Galdabini, Italy). The photoluminescence (PL) spectra of the films were measured at room temperature by a Hitachi F-4500 spectrophotometer using a Xe lamp as an excitation source. The resolution of the monochromater was 5 nm.

3. Results and discussion

3.1. Film formation and morphology

The freestanding SiC films of thickness ranging from 8 μm to 190 μm measured from the SEM micrographs of the cross-sections and without notable defect could be obtained in this study. The thickness of the films mainly depended on the spout size of the spinneret mouth and the ratio of spinning speed to extrusion rate. Fig. 1 shows the relationship between the thickness of the films and the spout size of the spinneret mouth and the spinning speed at a steady extrusion rate of 0.3 mm/min. Fig. 1(a) revealed the thickness of the films increased linearly with increasing spout size of the spinneret mouth. Fig. 1(b) shows the thickness of the films as a function of the spinning speed, and the thickness was inversely proportional to the spinning speed. Therefore, the result meant that the thickness could be controlled via these conditions.

The continuous freestanding PCS green films wound on a coil was showed in Fig. 2(c). The SEM examination of the surface and cross-section of green and pyrolyzed freestanding films were showed in Fig. 3. The figures indicated that the surface of the films were smooth, uniform, and dense. Few flaws presented in the films under high magnification (greater than 10,000×) might result from the decomposition of amorphous Si*Ox*C*y* with evaporation of gaseous SiO and CO at a temperature above 1000 °C,

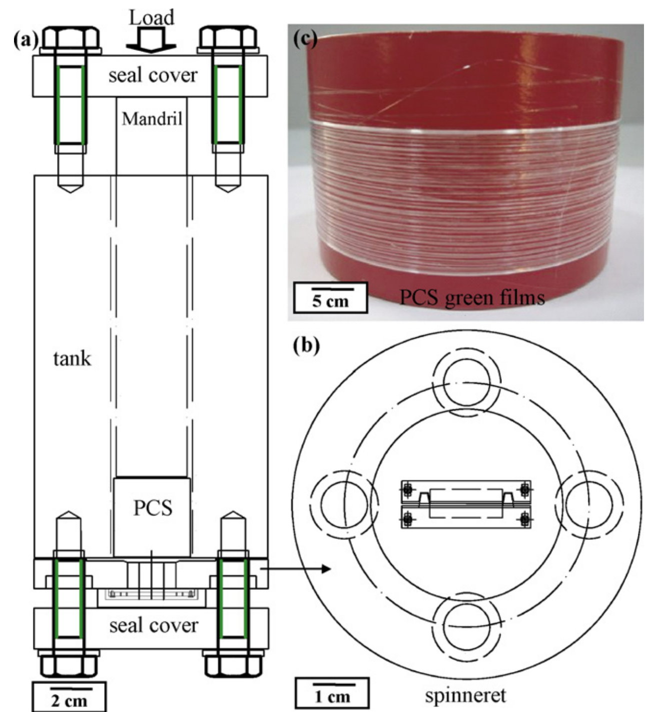

Fig. 2. Cross-section of the setup for melt spinning of continuous freestanding PCS films. (a) Side view of melt spinning device; (b) top view of spinneret and (c) image of PCS green films.

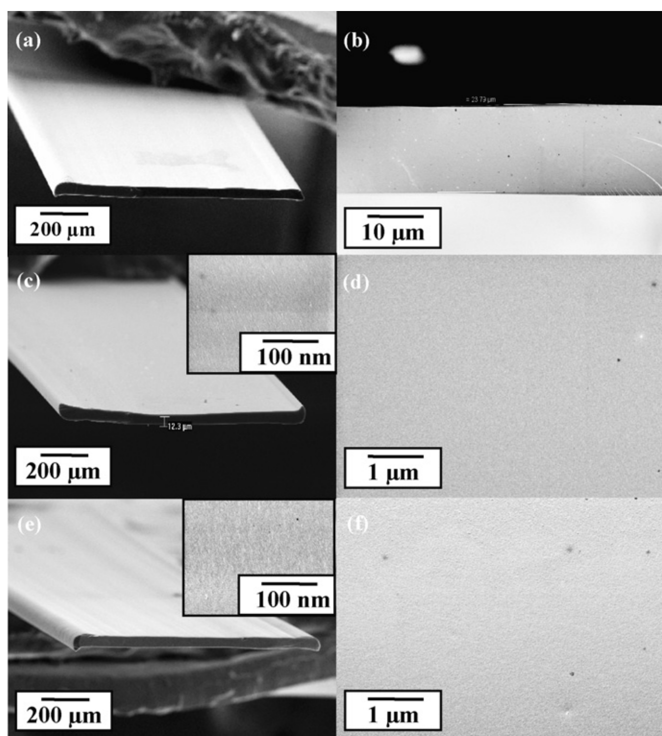

Fig. 3. SEM images of freestanding SiC films. (a) PCS green film; (b) cross-section of PCS green film; (c) pyrolyzed SiC film with oxidation and its cross-section enlargement; (d) surface of pyrolyzed SiC film with oxidation; (e) pyrolyzed SiC film with irradiation and its cross-section enlargement and (f) surface of pyrolyzed SiC film with irradiation.

main reaction included the following[29]:

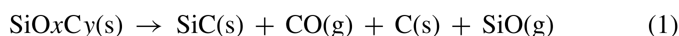

$$SiO_xC_y(s) \rightarrow SiC(s) + CO(g) + C(s) + SiO(g) \quad (1)$$

3.2. Compositional and structural analysis

The FTIR spectra in Fig. 4 had been collected for the green film, and films cured by oxidation and irradiation (peaks at

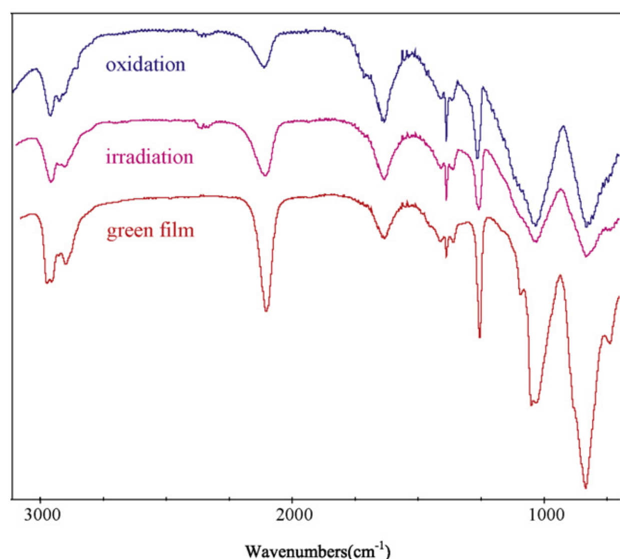

Fig. 4. FTIR spectra for continuous freestanding SiC films.

Table 1
Compositions and properties of continuous freestanding SiC films.

Film properties	Film with oxidation	Film with irradiation
Thickness/μm	19.35 ± 0.87	19.41 ± 0.93
Density/g cm^{-3}	2.58	2.69
Modulus/GPa	248	265
Hardness/GPa	10.94	11.65
Resistivity/Ω cm	10^4 to 10^5	32.56
Shrinkage/%	26.23	25.96
Elemental composition		
Si/wt%	56.6	57.3
C/wt%	30.1	38.4
O/wt%	13.3	4.3
n(C)/n(Si)	1.24	1.31

2950 cm^{-1} and 2900 cm^{-1}, due to C–H stretching of Si–CH_3, at 2100 cm^{-1}, due to Si–H stretching, at 1250 cm^{-1}, due to Si–CH_3 symmetric deformation, and at 1020 cm^{-1}, due to Si–C–Si stretching of Si–CH_2–Si).[8,12] The FTIRs exhibited increased SiC character due to crosslinking of terminal Si–H and Si–CH_3 groups, which was consistent with the loss of hydrogen (cleaving of the C–H and Si–H bonds in the PCS) that was observed. The spectra showed that the adsorption peak of Si–H in the film cured with oxidation was lower than that with irradiation. The presence of Si–H, Si–CH_2–Si, Si–O–Si, and Si–CH_3 modes in their spectra, together with the measured stoichiometric ratios, suggested the formation of –[SiH(CH_3)–O]$_3$–SiH(CH_3)–C– chains with Si–C–Si links between them.

The oxidation-induced curing mainly resulted in the crosslinking with oxygen of terminal Si–H and Si–CH_3 groups in the PCS, which formed Si–O–Si and Si–CH_2OOH bonds. However, in the case of EB irradiation, Si–H and Si–CH_3 groups in PCS reacted with neighboring chains to form a new bonding of Si–CH_2–Si between PCS chains. In addition, a part of Si–H groups reacted with each other to form Si–Si bonds. After curing, the films were converted to SiC using heat treatment. The pyrolysis reaction mechanism from the organic PCS to ceramic SiC consisted of the debonding reaction of Si–H and Si–CH_3 at 500–900 °C, and the decomposition of C–H bonds in Si–CH_2–Si above 900 °C.[27–29]

The composition of the pyrolyzed freestanding SiC films with oxidation and irradiation were shown in Table 1. The chemical concentrations were all measured by EPMA. As expected, it clearly appeared that the oxygen content of the EB-cured films was significantly lower than that of the oxygen-cured films originated from the PCS precursor used which was pre-oxidized in its as-received state. Both the films contained high amounts of free carbon. The EB-cured films generally had a slightly higher free carbon amount than that of oxygen-cured films. This feature was probably due to the much lower amounts of carbon atoms engaged in the rare or nearly absent SiO_xC_y phase in the former films.[27,28]

Fig. 5(a) shows the typical X-ray diffraction (XRD) patterns of pyrolyzed SiC films with oxidation-induced crosslinking and EB irradiation. The XRD patterns using Cu Kα of the as-received SiC-based films showed three main peaks which were assigned to the (1 1 1) ($2\theta = 35.528°$), (2 2 0) ($2\theta = 59.862°$) and

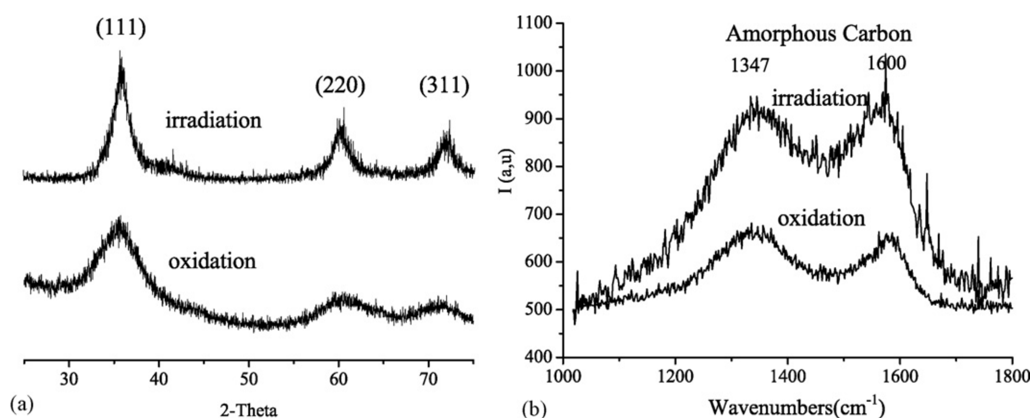

Fig. 5. (a) XRD of continuous freestanding SiC films and (b) Raman spectra of continuous freestanding SiC films.

(3 1 1) ($2\theta = 71.758°$) planes of β-SiC phase. The XRD peaks of SiC films by irradiation were apparently sharper than that by oxidation. The average crystallite sizes of β-SiC grains in the oxygen-cured and EB-cured films had been calculated to be 3.2 nm and 4.5 nm using the Scherrer equation, which was calculated from the half-value width of the (1 1 1) peak, respectively. The result indicated that β-SiC grain in the SiC films cured with irradiation grew into larger crystals than that with oxidation.

The Raman spectra investigation on films was present in this study. Fig. 5(b) shows the Raman spectra of pyrolyzed SiC films with oxidation-induced crosslinking and EB irradiation. The intensity of the peaks at $1347\,\mathrm{cm}^{-1}$ and $1600\,\mathrm{cm}^{-1}$ was proportional to the amount of free carbon in the films.[12,13] These peaks were rather wide, which indicated structural and chemical short-range disorder. It was revealed that the peak value of films with irradiation was larger than that with the oxidation. So a large proportion of the carbon atoms in irradiated films segregated into clusters during pyrolysis.

The TEM analysis (Fig. 6) very clearly showed that the main phases of continuous freestanding SiC films were amorphous SiO*x*C*y*. According to XRD and Raman spectroscopy analysis, β-SiC nano-crystals did not appear in the images, due to their tiny sizes less than 5 nm.[30,31] Thus, they were embedded within amorphous SiO*x*C*y* and free carbon. The electron diffraction pattern of films cured with irradiation (Fig. 6(b)) showed microcrystallites of β-SiC, the broaden rings corresponding to the (1 1 1), (2 2 0) and (3 1 1) Bragg reflections of β-SiC, whereas Fig. 5(b) shows the amorphous structure. This result indicated the β-SiC nano-crystals size in the pyrolyzed film with irradiation was larger than that with oxidation. Moreover, the film also contained a lower percentage of amorphous SiO*x*C*y* than oxidation.

3.3. Physical properties

The continuous freestanding SiC films of approximately 20 μm in thickness were selected to character their physical properties. This dimension suited for MEMS and optoelectronic devices applications.[10–16,25,32]

The resistance was directly measured at room temperature by means of an (HP16047A) test fixture. The results were shown in Table 1 for the continuous freestanding SiC films with oxidation and irradiation. The resistance of the oxygen-cured films was $10^4\,\Omega\,\mathrm{cm}$ to $10^5\,\Omega\,\mathrm{cm}$, and the value was about 3–4 orders of magnitude higher than the EB-cured films. Both the films showed a typical semi-conducting behavior. Considering that the films consisted mainly amorphous SiO*x*C*y*, β-SiC nano-crystals and free carbon, Such a value of electrical conductivity strongly suggested that the component controlling the electrical behavior was mainly the free carbon phase.[33] Because of the higher volume ratio of the free carbon phase to β-SiC in the EB-cured films, such value of electrical conductivity consistent to that of carbon materials suggested a continuous texture of the free carbon phase throughout the films. And the free carbon could form conducting domains. So the resistance value of the EB-cured films was lower than that of the oxygen-cured films.

The hardness of continuous freestanding SiC films was measured at room temperature with a microhardness tester. The hardness of the oxygen-cured films and EB-cured films was 10.94 GPa and 11.65 GPa, respectively. The room temperature elastic modulus for both films measured by a materials tester, were 248 GPa and 265 GPa, according to American Society of Testing Materials (ASTM D3379-75). The density was measured by a pressure-of-flotation method (PFM). The estimated density of oxygen-cured films was $2.58\,\mathrm{g\,cm}^{-3}$, and the value was smaller than that of EB-cured films ($2.69\,\mathrm{g\,cm}^{-3}$). The shrinkage of the film was reported as[12]

$$\text{shrinkage}\,(\%) = \left(\frac{t_0 - t}{t_0}\right) \times 100$$

where t_0 was the initial film thickness and t was the final film thickness after pyrolysis. The shrinkage upon pyrolysis of the oxygen-cured films and EB-cured films were 26.23% and 25.96%, respectively.

3.4. Photoluminescence properties

Fig. 7 depicted the room temperature PL spectra of the pyrolyzed SiC films with oxidation-induced crosslinking and EB irradiation, respectively. The spectra were acquired under 375 nm excitation of a Xe lamp. The PL spectra of films appeared in the visible light range and had a broad spectra feature with two blue peaks at 416 nm (3.01 eV) and 435 nm (2.88 eV), which

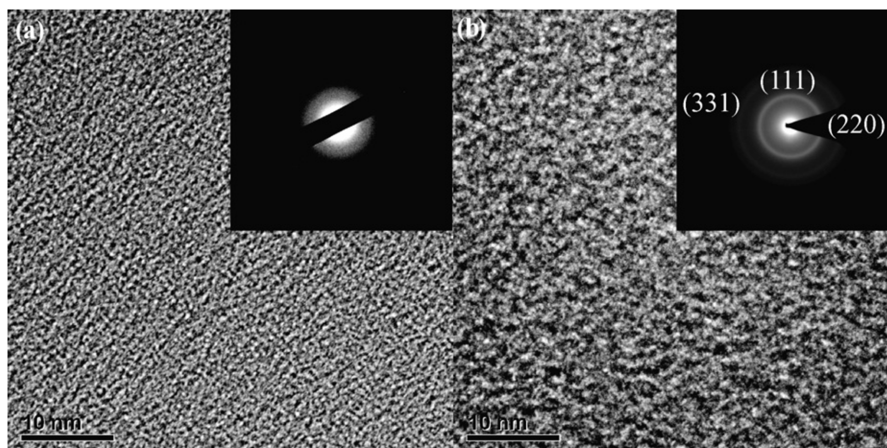

Fig. 6. TEM and electron diffraction pattern images of continuous freestanding SiC films. (a) pyrolyzed SiC film with oxidation and (b) pyrolyzed SiC film with irradiation.

were far above the band gap energy of the bulk β-SiC (2.30 eV). Comparing PL spectra of oxygen-cured films with EB-cured films, it was revealed that their positions almost kept unchanged, their intensities had large difference. The PL intensity (integral intensity) from the former was larger than that from the later.

PL consisted of three processes, which were photo-excitation, energy transmission and radiative recombination of the electron–hole pairs, respectively. Though different sizes of β-SiC nano-crystals existed in the two films, no position shift of the PL peaks illustrated that the blue double-peak PL was not from band to band recombination in the quantum confined β-SiC nano-crystals or quantum size effects.[34] Thus, the origin of PL centered at 416 nm and 435 nm might be related to the states at the surfaces of β-SiC nano-crystals, possibly a state of Si–Ox related defects.[34–36]

The amorphous SiOxCy consisted of mixed bonds of Si–O–C tetrahedral which contained abundant Si–Ox.[9,12,33] For the β-SiC films, the surface models had also been adopted to elucidate the blue light-emitting properties related to the β-SiC nano-crystals.[34,35] The photoexcited free electrons could tunnel through the surface of β-SiC nano-crystals and induce radiative recombination with Si–Ox related defects.[34,36–38]

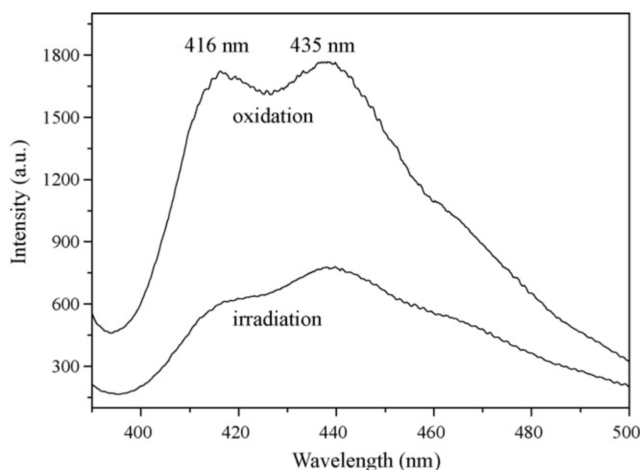

Fig. 7. Photoluminescence spectrum for continuous freestanding SiC films.

Above-mentioned reports and this study indicated that the PL property was affected by the presence of Si–O–C tetrahedral, and the two blue PL peaks arised from the Si–Ox bonds formation. The intensity of Si–Ox bonds and that of PL were enhanced simultaneously with the increase of oxygen content. Moreover, the specific surface area of β-SiC nano-crystals in the oxygen-cured films was larger than that of the EB-cured films, due to the smaller grain size distribution. Therefore, the PL intensity from the former was larger than that from the later. Recently some researchers also ascribed the peak at 416 nm to the C clusters.[6] However, further experimental and the theoretical investigations were needed to address this issue. In addition, their thermal, mechanical, electrical and optical properties still needed further research.

4. Conclusions

In this investigation, the dense and continuous freestanding SiC films were first synthesized using the novel technique of melt spinning of PCS precursor. An equipment consisted of spinneret, mandril, tank, seal cover and seal groove was successfully set up for melt spinning. In comparison with spin-coating process using PCS on Si substrates, the freestanding films could avoid mismatches of thermal expansion coefficient and lattice constant at the interface between SiC coatings and substrate.

The microstructure of the freestanding films consisted of amorphous SiOxCy, β-SiC nano-crystals and free carbon. The thickness of the films ranged from 8 μm to 190 μm depending on the spout size of spinneret mouth and spinning speed. Results revealed that green freestanding films could be cured with oxidation-induced crosslinking or EB irradiation. The continuous freestanding SiC films may be promising in the applications such as MEMS, source of blue light, advanced optoelectronic devices and such complex-shaped materials.

Acknowledgement

This work is supported by the National Natural Science Foundation of China (Grant No. 50532010).

References

1. Brutsch, R., Chemical vapor deposition of silicon carbide and its applications. *Thin Solid Films*, 1985, **126**, 313–318.
2. Golecki, I., Reidinger, F. and Marti, J., Single-crystalline, epitaxial cubic SiC films grown on (1 0 0) Si at 750 °C by chemical vapor deposition. *Appl. Phys. Lett.*, 1992, **60**(14), 1703–1705.
3. Colombo, P., Martucci, A., Fogato, O. and Villoresi, P., Silicon carbide films by laser pyrolysis of polycarbosilane. *J. Am. Ceram. Soc.*, 2001, **84**(1), 224–226.
4. Feng, Z. C., Second order Raman scattering of cubic silicon carbide. In *Proceedings of the XIXth International Conference on Raman Spectroscopy*, ed. P. M. Fredericks, R. L. Frost and L. Rintoul. CSIRO Publishing, Gold Coast, Queensland, Australia, 2004, pp. 242–243.
5. Katharria, Y. S., Kumar, S., Prakash, R., Choudhary, R. J., Singh, F., Phase, D. M. and Kanjilal, D., Characterizations of pulsed laser deposited SiC thin films. *J. Non-Cryst. Solids*, 2007, **353**(52–54), 4660–4665.
6. Sha, Z. D., Wu, X. M. and Zhuge, L. J., Initial study on the structure and photoluminescence properties of SiC films doped with Al. *Appl. Surf. Sci.*, 2006, **252**(12), 4340–4344.
7. Polychroniadis, E., Syvajarvi, M., Yakimova, R. and Stoemenos, J., Microstructural characterization of very thick freestanding 3C–SiC wafers. *J. Cryst. Growth*, 2004, **263**(1–4), 68–75.
8. Yajima, S., Hayashi, J. and Omori, M., Continuous silicon carbide fibers of high tensile strength. *Chem. Lett.*, 1975, **9**, 931–934.
9. Yajima, S., Hasegawa, Y., Okamura, K. and Matsuzawa, T., Development of high tensile strength silicon carbide fiber using an organosilicon polymer precursor. *Nature*, 1978, **273**(5663), 525–527.
10. Chu, C.-J., Soraru, G. D., Babonneau, F. and Mackenzie, J. D., Preparation and characterization of amorphous SiC film by a liquid route. In *Springer Proceedings in Physics, vol. 43, Amorphous and Crystalline Silicon Carbide and Related Materials II*, ed. M. M. Rahman and G. L. Harris. Springer-Verlag, Berlin, FRG, 1989, pp. 66–71.
11. Chu, C.-J., Liimatta, E. and Mackenzie, J. D., Doped amorphous SiC, mixed carbide and oxycarbide thin films by a liquid route. *Mater. Res. Soc. Symp. Proc.*, 1990, **162**, 421–426.
12. Colombo, P., Paulson, T. E. and Pantano, C. G., Synthesis of silicon carbide thin films with polycarbosilane (PCS). *J. Am. Ceram. Soc.*, 1997, **80**(9), 2333–2340.
13. Pivin, J. C., Colombo, P. and Soraru, G. D., Comparison of ion irradiation effects in silicon-based preceramic thin films. *J. Am. Ceram. Soc.*, 2000, **83**(4), 713–720.
14. Stark, B., *MEMS Reliability Assurance Guidelines for Space Applications*. Jet. Propulsion Laboratory, NASA, JPL Publication, 1999, pp. 69–90.
15. Nagasawa, H. and Yagi, K., 3C–SiC single crystal films grown on 6-inch Si substrates. *Phys. Stat. Sol. B*, 1997, **202**(1), 335–358.
16. Yang, H., Deschatelets, P., Brittain, S. T. and Whitesides, G. M., Fabrication of high performance ceramic microstructures from a polymeric precursor using soft lithography. *Adv. Mater.*, 2001, **13**(1), 54–58.
17. Chung, G.-S., Characteristics of SiCN microstructures for harsh environment and high-power MEMS applications. *Microelectron. J.*, 2007, **38**(8–9), 888–893.
18. Hanemann, T., Ade, M., Borner, M., Motz, G., Schulz, M. and Hausselt, J., Microstructuring of preceramic polymers. *Adv. Eng. Mater.*, 2002, **4**(11), 869–873.
19. Liew, L.-A., Zhang, W. G., An, L. N., Shah, S., Luo, R. L., Liu, Y. P., Cross, T., Dunn, M. L., Bright, V., Daily, J. W., Raj, R. and Anseth, K., Ceramic MEMS—new materials, innovative processing and future applications. *Am. Ceram. Soc. Bull.*, 2001, **80**(5), 25–30.
20. Liew, L.-A., Liu, Y. P., Luo, R. L., Cross, T., An, L. N., Bright, V. M., Dunn, M. L., Daily, J. W. and Raj, R., Fabrication of SiCN MEMS by photopolymerization of pre-ceramic polymer. *Sens. Actuators A-Phys.*, 2002, **95**(2–3), 120–134.
21. Liew, L.-A., Bright, V. M. and Raj, R., A novel micro glow plug fabricated from polymer-derived ceramics: in situ measurement of high-temperature properties and application to ultrahigh-temperature ignition. *Sens. Actuators A-Phys.*, 2003, **104**(3), 246–262.
22. Liew, L.-A., Saravanan, R. A., Bright, V. M., Dunn, M. L., Daily, J. W. and Raj, R., Processing and characterization of silicon carbon-nitride ceramics: application of electrical properties towards MEMS thermal actuators. *Sens. Actuators A-Phys.*, 2003, **103**(1–2), 171–181.
23. Schulz, M., Borner, M., Gottert, J., Hanemann, T., Hausselt, J. and Motz, G., Cross-linking behavior of preceramic polymers effected by UV- and synchrotron radiation. *Adv. Eng. Mater.*, 2004, **6**(8), 676–680.
24. Schulz, M., Borner, M., Hausselt, J. and Heldele, R., Polymer derived ceramic microparts from X-ray lithography: cross-linking behavior and process optimization. *J. Eur. Ceram. Soc.*, 2005, **25**(2–3), 199–204.
25. Pham, T. A., Kim, D.-P., Lim, T.-W., Park, S.-H., Yang, D.-Y. and Lee, K.-S., Three-dimensional SiCN ceramic microstructures via nano-stereolithography of inorganic polymer photoresists. *Adv. Funct. Mater.*, 2006, **16**(9), 1235–1241.
26. Lee, H.-J., Yoon, T.-H. and Kim, D.-P., Fabrication of microfluidic channels derived from a UV/thermally cured preceramic polymer via a soft lithographic technique. *Microelectron. Eng.*, 2007, **84**(12), 2892–2895.
27. Okamura, K. and Seguchi, T., Application of radiation curing in the preparation of polycarbosilane-derived SiC fibers. *J. Inorg. Organomet. Polym.*, 1992, **2**(1), 171–179.
28. Youngblood, G. E., Jones, R. H., Kohyama, A. and Snead, L. L., Radiation response of SiC-based fibers. *J. Nucl. Mater.*, 1998, **258–263**, 1551–1556.
29. He, G. W., Shibayama, T. and Takahashi, H., Microstructural evolution of Hi-Nicalon^{TM} SiC fibers annealed and crept in various oxygen partial pressure atmospheres. *J. Mater. Sci.*, 2000, **35**(5), 1153–1164.
30. Kleebe, H.-J., Braue, W., Schmidt, H., Pezzotti, G. and Ziegler, G., Transmission electron microscopy of microstructures in ceramic materials. *J. Eur. Ceram. Soc.*, 1996, **16**(3), 339–351.
31. Nakano, H., Watari, K., Kinemuchi, Y., Ishizaki, K. and Urabe, K., Microstructural characterization of high-thermal-conductivity SiC ceramics. *J. Eur. Ceram. Soc.*, 2004, **24**(14), 3685–3690.
32. Mehregany, M. and Zorman, C. A., SiC MEMS: opportunities and challenges for applications in harsh environments. *Thin Solid Films*, 1999, **355–356**, 518–524.
33. Chollon, G., Pailler, R., Canet, R. and Delhaes, P., Correlation between microstructure and electrical properties of SiC-based fibers derived from organosilicon precursors. *J. Eur. Ceram. Soc.*, 1998, **18**(6), 725–733.
34. Tan, C., Wu, X. L., Deng, S. S., Huang, G. S., Liu, X. N. and Bao, X. M., Blue emission from silicon-based β-SiC films. *Phys. Lett. A*, 2003, **310**(2–3), 236–240.
35. Das, G., Bettotti, P., Ferraioli, L., Raj, R., Mariotto, G., Pavesi, L. and Soraru, G. D., Study of the pyrolysis process of an hybrid $CH_3SiO_{1.5}$ gel into a SiCO glass. *Vib. Spectrosc.*, 2007, **45**(1), 61–68.
36. Pivin, J. C. and Sendova-Vassileva, M., Visible photoluminescence of ion irradiated polysiloxane films. *Solid State Commun.*, 1998, **106**(3), 133–138.
37. Pivin, J. C., Colombo, P., Martucci, A., Soraru, G. D., Pippel, E. and Sendova-Vassileva, M., Ion beam induced conversion of Si-based polymers and gels layers into ceramics coatings. *J. Sol-Gel Sci. Technol.*, 2003, **26**(1–3), 251–255.
38. Ferraioli, L., Ahn, D., Saha, A., Pavesi, L. and Raj, R., Intensely photoluminescent pseudo-amorphous SiliconOxyCarboNitride polymer-ceramic hybrids. *J. Am. Ceram. Soc.*, 2008, **91**(7), 2422–2424.